

## Ion channels in human erythroblasts. Modulation by erythropoietin.

J Y Cheung, ... , D L Tillotson, B A Miller

*J Clin Invest.* 1992;**90**(5):1850-1856. <https://doi.org/10.1172/JCI116061>.

### Research Article

To investigate the mechanism of intracellular  $\text{Ca}^{2+}$  ( $[\text{Ca}^{2+}]_i$ ) increase in human burst-forming unit-erythroid-derived erythroblasts by erythropoietin, we measured  $[\text{Ca}^{2+}]_i$  with digital video imaging, cellular phosphoinositides with high performance liquid chromatography, and plasma membrane potential and currents with whole cell patch clamp. Chelation of extracellular free  $\text{Ca}^{2+}$  abolished  $[\text{Ca}^{2+}]_i$  increase induced by erythropoietin. In addition, the levels of inositol-1,4,5-trisphosphate did not increase in erythropoietin-treated erythroblasts. These results indicate that in erythropoietin-stimulated cells,  $\text{Ca}^{2+}$  influx rather than intracellular  $\text{Ca}^{2+}$  mobilization was responsible for  $[\text{Ca}^{2+}]_i$  rise. Both  $\text{Ni}^{2+}$  and moderately high doses of nifedipine blocked  $[\text{Ca}^{2+}]_i$  increase, suggesting involvement of ion channels. Resting membrane potential in human erythroblasts was  $-10.9 \pm 1.0$  mV and was not affected by erythropoietin, suggesting erythropoietin modulated a voltage-independent ion channel permeable to  $\text{Ca}^{2+}$ . No voltage-dependent ion channel but a  $\text{Ca}^{2+}$ -activated  $\text{K}^+$  channel was detected in human erythroblasts. The magnitude of erythropoietin-induced  $[\text{Ca}^{2+}]_i$  increase, however, was insufficient to open  $\text{Ca}^{2+}$ -activated  $\text{K}^+$  channels. Our data suggest erythropoietin modulated a voltage-independent ion channel permeable to  $\text{Ca}^{2+}$ , resulting in sustained increases in  $[\text{Ca}^{2+}]_i$ .

Find the latest version:

<https://jci.me/116061/pdf>



# Ion Channels in Human Erythroblasts

## Modulation by Erythropoietin

Joseph Y. Cheung, MaryBeth Elensky, Ulrike Brauneis, Russell C. Scaduto, Jr.,  
Laurie L. Bell, Douglas L. Tillotson, and Barbara A. Miller

Departments of Medicine, Cellular and Molecular Physiology, and Pediatrics, The Milton S. Hershey Medical Center, The Pennsylvania State University, Hershey, Pennsylvania 17033; and Department of Physiology, Boston University School of Medicine, Boston, Massachusetts 02118

### Abstract

To investigate the mechanism of intracellular  $\text{Ca}^{2+}$  ( $[\text{Ca}]_i$ ) increase in human burst-forming unit-erythroid-derived erythroblasts by erythropoietin, we measured  $[\text{Ca}]_i$  with digital video imaging, cellular phosphoinositides with high performance liquid chromatography, and plasma membrane potential and currents with whole cell patch clamp. Chelation of extracellular free  $\text{Ca}^{2+}$  abolished  $[\text{Ca}]_i$  increase induced by erythropoietin. In addition, the levels of inositol-1,4,5-trisphosphate did not increase in erythropoietin-treated erythroblasts. These results indicate that in erythropoietin-stimulated cells,  $\text{Ca}^{2+}$  influx rather than intracellular  $\text{Ca}^{2+}$  mobilization was responsible for  $[\text{Ca}]_i$  rise. Both  $\text{Ni}^{2+}$  and moderately high doses of nifedipine blocked  $[\text{Ca}]_i$  increase, suggesting involvement of ion channels. Resting membrane potential in human erythroblasts was  $-10.9 \pm 1.0$  mV and was not affected by erythropoietin, suggesting erythropoietin modulated a voltage-independent ion channel permeable to  $\text{Ca}^{2+}$ . No voltage-dependent ion channel but a  $\text{Ca}^{2+}$ -activated  $\text{K}^+$  channel was detected in human erythroblasts. The magnitude of erythropoietin-induced  $[\text{Ca}]_i$  increase, however, was insufficient to open  $\text{Ca}^{2+}$ -activated  $\text{K}^+$  channels. Our data suggest erythropoietin modulated a voltage-independent ion channel permeable to  $\text{Ca}^{2+}$ , resulting in sustained increases in  $[\text{Ca}]_i$ . (*J. Clin. Invest.* 1992. 90:1850–1856.) Key words: Fura-2 • digital video imaging • fluorescence microscopy • patch-clamp •  $\text{Ca}^{2+}$ -activated  $\text{K}^+$  channels

### Introduction

Signal transduction by erythropoietin (Epo)<sup>1</sup> involves a series of biochemical and ionic regulatory events. After erythropoietin stimulation of erythroid cells, increased intracellular free calcium (1–3), increased cAMP levels (4, 5), and activation of protein kinases (6) have been reported to occur. Evidence suggests that these may follow activation of a GTP-binding protein

1. *Abbreviations used in this paper:* ANOVA, analysis of variance; BFU-E, burst-forming unit-erythroid;  $[\text{Ca}]_i$ , intracellular  $\text{Ca}^{2+}$ ; Epo, erythropoietin;  $\text{IP}_3$ , inositol-1,4,5-trisphosphate.

Address correspondence to Joseph Y. Cheung, M.D., Ph.D., Division of Nephrology, Department of Medicine, The Milton S. Hershey Medical Center, P.O. Box 850, Hershey, PA 17033.

Received for publication 24 March 1992 and in revised form 8 June 1992.

*J. Clin. Invest.*

© The American Society for Clinical Investigation, Inc.

0021-9738/92/11/1850/07 \$2.00

Volume 90, November 1992, 1850–1856

by the receptor (5, 7). Signals transmitted to the nucleus include increased nuclear calcium (8), activation of nuclear protein kinase C (9), and change in protooncogene expression (10–12). The precise sequence of events that follow hormone/receptor interaction and control erythroid proliferation and subsequent differentiation is undefined.

We have previously shown that Epo induces a dose-dependent increase in intracellular calcium ( $[\text{Ca}]_i$ ) in single human burst-forming unit-erythroid (BFU-E)-derived erythroblasts (1), which is specific for stage of differentiation (2), and that  $\text{Ca}^{2+}$  increase is transmitted to the nucleus (8). The current study was undertaken to investigate the mechanism by which Epo stimulates the increase in  $[\text{Ca}]_i$ . Specifically, the influence of Epo on ionic permeabilities was evaluated. To better elucidate the regulation of membrane voltage and ion currents, we applied, for the first time, whole cell patch-clamp technique to human BFU-E-derived erythroblasts.

### Methods

*Preparation of BFU-E-derived erythroid precursors.* Adult blood was obtained according to a protocol approved by the Milton S. Hershey Medical Center Committee on Clinical Investigation. Adult blood BFU-E were partially purified by 2-aminoethylisothiuronium bromide hydrobromide-treated sheep red blood cell (RBC) rosetting, adherence to plastic, and panning, as described previously (1, 2). Partially purified mononuclear cells from adult blood were cultured in humidified 4%  $\text{CO}_2$  at 37°C in 0.9% methylcellulose media containing 30% FCS, 9.0 mg/ml deionized BSA (fraction V; Sigma Chemical Co., St. Louis, MO),  $1.4 \times 10^{-4}$  mol/liter  $\beta$ -mercaptoethanol, 2 U/ml recombinant Epo ( $> 10,000$  U/mg) (Amgen Biologicals, Thousand Oaks, CA), and recombinant granulocyte macrophage colony-stimulating factor (gift of Dr. Steven Clark; Genetics Institutes, Cambridge, MA; 25 ng/ml final concentration). Concentrations of Epo and granulocyte macrophage-colony-stimulating factor were selected for plateau stimulation of growth (2).

To study erythroid precursors at specific stages of differentiation, cells from maturing BFU-E-derived colonies were plucked from culture on day 10. Day 10 cells are partially hemoglobinized and proliferative capacity is decreased since minimal additional increase in colony size occurs subsequently. Myeloid colonies represented  $< 1\%$  of hematopoietic colonies cultured from partially purified PBMC prepared as described.

*Measurement of  $[\text{Ca}]_i$  in early erythroid precursor cells.* BFU-E-derived cells were removed from culture on day 10 and labeled with plateau concentrations of anti-human  $\beta_2$ -microglobulin (Chemicon International, Inc., Temecula, CA). Cells were then bound to anti-mouse Ig-coated glass coverslips by incubating at 4°C for 1 h. The cells were incubated in PBS (Table I) at 37°C for 20 min with 1  $\mu\text{mol/liter}$  Fura-2 acetoxymethyl ester (Molecular Probes, Inc., Eugene, OR). Total time lapse from removal of cells from culture to completion of Fura-2 loading was 3–5 h. Cell viability, as judged by trypan blue exclusion, was  $> 98\%$ . Baseline  $[\text{Ca}]_i$  and its changes in response to Epo (2

Table I. Composition of Bath and Pipette Solutions

Solution	pH	NaCl	KCl	KASP	CsCl	MgCl <sub>2</sub>	CaCl <sub>2</sub>	EGTA	ATP	GTP	Hepes
<b>Bath</b>											
PBS	7.4	137	2.7			0.49	0.68				
EGTA	7.4	137	2.7			0.49	0.68	4			
CsCl	7.4	137			3.4	0.49	0.68				
KASP	7.2	5		140		2	2				10
<b>Filling</b>											
Normal	7.0	5	125			2		1	2		20
CsCl	7.0	5			125	2		1	2		20
KASP	7.2	5		140		2		0.2	1	0.02	10

All concentrations are millimolar. All bath solutions contained 200 mg/dl glucose. PBS and EGTA also contained 4.3 mM Na<sub>2</sub>HPO<sub>4</sub> and 1.5 mM KH<sub>2</sub>PO<sub>4</sub>. Bath CsCl solution contained 7.2 mM Na<sub>2</sub>HPO<sub>4</sub>.

U/ml) in Fura-2-loaded cells incubated in either PBS with physiologic calcium (0.7 mM) or PBS without calcium (2 mM EGTA) were measured with the fluorescence microscopy-coupled digital video imaging system as described previously (1, 2, 5, 8). Cells were chosen based on visible Fura-2 fluorescence and normal cellular morphology (round cytoplasmic borders and absence of cytoplasmic vacuoles) by light microscopy (8). More than 90% of the cells on coverslips met these criteria. The dose of Epo was chosen to elicit maximal [Ca<sub>i</sub>] response both in terms of amplitude of [Ca<sub>i</sub>], as well as the percentage of cells with significant [Ca<sub>i</sub>] increase over baseline (1, 2). [Ca<sub>i</sub>] was calculated from ratiometric fluorescence images of Fura-2 loaded cells by the in vivo calibration method (2), using 224 nM as the K<sub>d</sub> for Ca<sup>2+</sup>-Fura-2 complex (13). It should be noted that using our Fura-2 loading protocol, we have previously shown that [Ca<sub>i</sub>] values derived from the Fura-2-free acid calibration curve (in vitro calibration) and from the in vivo calibration method are indistinguishable (2).

In some experiments, CaCl<sub>2</sub> (3 mM) or NiCl<sub>2</sub> (1 mM) was added at 10 min to PBS with or without Ca<sup>2+</sup> (2 mM EGTA). Where stated, cells were pretreated with nifedipine (1, 10, or 50 μM) for 3 min before addition of Epo.

**Measurement of cellular inositol phosphates.** Day 10 human BFU-E-derived erythroblasts were removed from culture and incubated overnight at 1.4 × 10<sup>6</sup> cells/ml, 37°C, in inositol-free Iscove's modified Dulbecco's media (IMDM) containing 20% dialyzed FCS and [2-<sup>3</sup>H]-myo-inositol (40 μCi) (American Radiolabeled Chemicals Inc., St. Louis, MO). Cells were washed, resuspended in inositol-free IMDM with 2% dialyzed FCS, and pretreated with lithium chloride (20 mM) for 15 min. The cell suspension was divided into two equal halves, and Epo (2 or 10 U/ml) was added to one of these halves. After 1, 5, or 10 min of incubation with Epo or its vehicle, equal volumes of 10% ice-cold TCA was added to quench the cell suspensions. After centrifugation (15,600 g), TCA was removed from the supernatant by four to five extractions with water-saturated diethylether. The supernatant was adjusted to pH 7–8 and stored frozen.

Inositol phosphates were separated on a 10 SAX column (Partisil; Whatman Inc., Clifton, NJ) with ammonium phosphate, pH 3–8, flow rate at 1 ml/min, as previously described (14, 15). Gradients used were 0.01–0.08 M over 30 min for [<sup>3</sup>H]inositol-1-phosphate, 0.2–0.28 M over 30 min for [<sup>3</sup>H]inositol-1,4-bisphosphate, 0.5–0.52 M over 30 min for [<sup>3</sup>H]inositol-1,4,5-trisphosphate, and 1 M over 30 min for [<sup>3</sup>H]inositol-1,3,4,5-tetrakisphosphate. Standards for [<sup>3</sup>H]inositol-mono-, bis-, and trisphosphates were purchased from Amersham Corp. (Arlington Heights, IL), and those for [<sup>3</sup>H]inositol-tetrakisphosphate were purchased from New England Nuclear (Boston, MA). Gradients were controlled with the Maxima 820 program (Waters Assoc. Inc., Milford, MA). A mixture of the above standards could be separated by applying the gradients described, collecting 1-ml fractions, and determining radioactivity by liquid scintillation counting (Fig. 3 A).

**Electrophysiological measurements.** Whole cell patch-clamp recordings were performed at room temperature and as described by Hamill et al. (16). Micropipettes were fabricated from borosilicate glass capillaries (No. 1B150-4; World Precision Instruments, Sarasota, FL) with a two-stage needle/pipette puller (model 750; David Kopf Instruments, Tujunga, CA) and typically had diameters of 1–2 μm. Pipettes were fire polished as described by Leibowitz and Dionne (17), after which they showed resistances of 14 ± 1 MΩ. For voltage clamping, current amplification, and current clamping, a patch-clamp amplifier (Axopatch-1C; Axon Instruments, Foster City, CA) with CV-4 1/100 headstage was used. For data acquisition and analysis, an IBM PC/AT computer interfaced with an IBX A/D and D/A converter (Indec Systems, Sunnyvale, CA) was used in conjunction with BASIC-FASTLAB software (Indec Systems).

After formation of GΩ seal (seal resistance 1.1–3.2 GΩ) by suction, pipette resistance was compensated by minimizing the duration of capacitive surge on the current trace. The patch membrane was then disrupted by applying 1.5 V DC to the patch for a controlled duration (ZAP function on Axopatch-1C). Reappearance of capacitive currents indicated that whole cell configuration had been attained. Cell capacitance and series resistance were compensated with analogue circuitry of the patch-clamp amplifier. Currents were filtered at 2 kHz and data acquired at 10 kHz. Voltages were referenced to the bath, i.e., positive voltage was depolarizing and negative voltage was hyperpolarizing. Outward current (positive current) represented flow of cations from cell to bath or anion flow from bath to cell.

Composition of different bath and pipette filling solutions are given in Table I. Pipette filling solutions were filtered with 0.22-μm filters (Millipore Corp., Bedford, MA) immediately before use. With PBS and normal filling solution, liquid junction potential (18) at the tip of electrode was 2.7 ± 0.3 mV, the potential inside the electrode being negative. Since this potential level was taken as reference potential, membrane potential values measured in current-clamp experiments would be at least 2.7 mV more negative than those reported here. No corrections were made, since the junction potentials between pipette filling solution and cytoplasm, and that between PBS and reference electrode (PBS and 1 M KCl in 2% agar), were unknown.

## Results

**Influence of extracellular calcium on the [Ca<sub>i</sub>] increase in response to erythropoietin.** To determine whether the increase in intracellular calcium measured in response to erythropoietin (1) originated from intracellular stores or external calcium, single day 10 BFU-E-derived erythroblasts loaded with Fura-2 were stimulated by Epo in the presence of physiologic calcium or its absence (2 mM EGTA). [Ca<sub>i</sub>] was measured over 20 min

**Table II. Effect of External Calcium on  $[Ca_i]$  Increase in Day 10 BFU-E-derived Erythroblasts Stimulated with Erythropoietin**

Stimulated with	External calcium	No. of cells	Basal $[Ca_i]$	Epo-induced peak $[Ca_i]$
			nM	nM
Epo	+	19	33±3	204±64*
Epo	-	12	26±4	30±5
PBS	+	16	22±3	25±4

Day 10 BFU-E-derived erythroblasts loaded with Fura-2 were stimulated with recombinant Epo (2 U/ml) or PBS (vehicle) in the presence of physiologic calcium (0.7 mM) or its absence (2 mM EGTA).  $[Ca_i]$  was measured over 20 min with fluorescence microscopy-coupled digital video imaging. Mean  $[Ca_i]$ ±SEM at baseline and the peak after 20 min of Epo stimulation are shown. Number of cells shown were from four experiments on different blood donors. Differences among means were tested with one-way ANOVA. A priori comparisons of means of baseline vs. Epo-treated groups were then performed using F tests as tests of significance. \* Significant increase above baseline ( $P < 0.001$ ).

with fluorescence microscopy-coupled digital video imaging. Results are shown in Table II.  $[Ca_i]$  significantly increased in the presence of physiologic calcium ( $P < 0.001$ ), but no increase was observed in the absence of external calcium. Calcium images of erythroblasts did not reveal redistribution of cell calcium in the absence of external  $Ca^{2+}$  (data not shown).

In another series of experiments, day 10 BFU-E-derived erythroblasts loaded with Fura-2 were stimulated with erythropoietin or PBS in the absence of external calcium (2 mM EGTA). Results are shown in Fig. 1. No change in  $[Ca_i]$  was

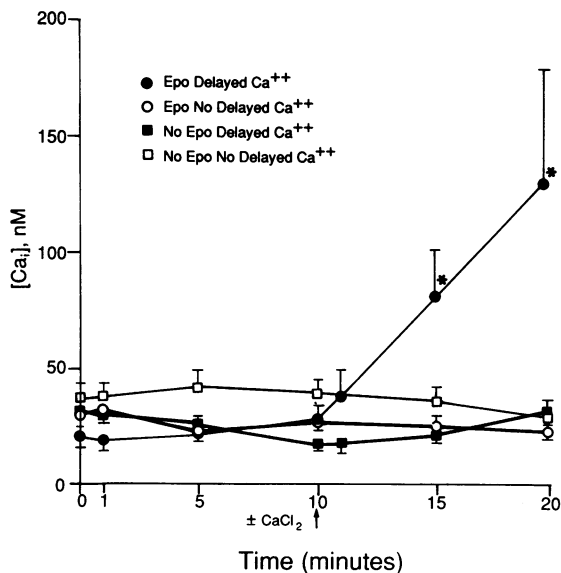


**Figure 1.** Effect of erythropoietin on  $Ca^{2+}$  permeability on human erythroblasts. Fura-2-loaded day 10 human BFU-E-derived erythroblasts were treated with Epo (2 U/ml) or PBS (vehicle) in 2 mM EGTA at 0 min. Exogenous calcium chloride (3 mM) was added to two groups at 10 min. Mean  $[Ca_i]$ ±SEM was measured over 20 min by digital video imaging. 9 (—○—), 14 (—■—), and 16 cells (—●—) were studied. \*Significant increase above baseline by one-way ANOVA ( $P < 0.05$ ).

observed over 20 min in the absence of extracellular free calcium. However, when calcium chloride (3 mM) was added at 10 min, there was a prompt increase in  $[Ca_i]$  from 28±7 to 131±49 nM in erythroblasts treated with erythropoietin at time 0. Addition of exogenous calcium to erythroblasts not primed with erythropoietin did not increase  $[Ca_i]$ . These results indicate that erythropoietin primed the  $Ca^{2+}$  influx pathway, which remained open so that when extracellular free  $Ca^{2+}$  was made available,  $[Ca_i]$  increased promptly.

**Influence of calcium channel blocking agents on the Epo-Induced Increase in  $[Ca_i]$ .** To explore the mechanism of  $Ca^{2+}$  entry, Fura-2 loaded day 10 BFU-E-derived cells were pretreated in the presence of external calcium (0.7 mM) for 3 min with the L-type  $Ca^{2+}$  channel blocker nifedipine (19) at concentrations of 1, 10, and 50  $\mu$ M. Cells were then stimulated with erythropoietin (2 U/ml) and  $[Ca_i]$  measured over 20 min. Results are shown in Table III. Nifedipine blocked the increase in  $[Ca_i]$  seen in response to erythropoietin, but only at doses higher than typically required to block voltage-sensitive L-type  $Ca^{2+}$  channels.

To examine if calcium influx is blockable after its activation by erythropoietin, day 10 BFU-E-derived erythroblasts were first treated with erythropoietin, and nickel chloride was added at 10 min after erythropoietin addition. As shown in Fig. 2, nickel chloride effectively reversed Epo-induced  $[Ca_i]$  increase even after the stimulatory effect of erythropoietin on  $Ca^{2+}$  influx was well established.

**Effects of erythropoietin on cellular inositol-1,4,5-trisphosphate levels.** BFU-E-derived erythroblasts labeled with  $[^3H]$ -myo-inositol were stimulated with Epo (2 or 10 U/ml) and cellular  $[^3H]$ inositol phosphates were measured. Because of the small number of BFU-E-derived erythroblasts, only control cells and one experimental group could be studied on any given day. Fig. 3 shows a representative experiment in which cells were stimulated by Epo (10 U/ml) for 5 min. No measurable increase in inositol-1,4,5-trisphosphate ( $IP_3$ ) level was observed after 1, 5, and 10 min ( $n = 2$  each) of Epo treatment. While the small  $[^3H]IP_3$  signals (Fig. 3, B and C) may have precluded us from detecting a 20–30% increase in  $IP_3$  in Epo-stimulated cells, it is unlikely that we would have missed a two- to three-

**Table III. Nifedipine Blocks the Epo-induced  $[Ca_i]$  Increase Observed in the Presence of Physiologic Calcium**

Pretreated with	Stimulated with	No. of cells	Basal $[Ca_i]$	Peak $[Ca_i]$
			nM	nM
IMDM	Epo	10	32±7	110±18*
Nif 1 $\mu$ M	Epo	5	41±9	79±10*
Nif 10 $\mu$ M	Epo	3	49±8	65±17
Nif 50 $\mu$ M	Epo	7	33±8	44±12
Nif 50 $\mu$ M	IMDM	3	18±5	16±2
IMDM	IMDM	5	29±6	49±20

Day 10 BFU-E-derived cells were pretreated with nifedipine (1, 10, or 50  $\mu$ M) or IMDM for 3 min in the presence of physiologic calcium (0.7 mM). Baseline  $[Ca_i]$  measurements were obtained and the cells were then stimulated with Epo (2 U/ml) or IMDM.  $[Ca_i]$  was measured over 20 min. Mean peak  $[Ca_i]$ ±SEM after stimulation is shown. \* Significant increase above baseline by one-way ANOVA ( $P < 0.05$ ).

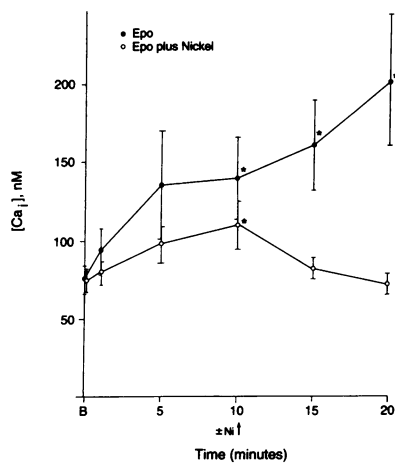


**Figure 2.** Nickel blocks erythropoietin-stimulated  $\text{Ca}^{2+}$  influx pathway. Fura-2-loaded day 10 human BFU-E-derived erythroblasts in PBS containing 0.67 mM  $\text{Ca}^{2+}$  were treated with Epo (2 U/ml) at 0 min. At 10 min, nickel chloride (1 mM) was added to one group of cells. Mean  $[\text{Ca}_i] \pm \text{SEM}$  was measured over 20 min by digital video imaging. 18 (—●—) and 19 (—○—) erythroblasts from six differ-

ent donors were studied. \*Significant increase above baseline ( $P < 0.05$ ).

fold increase commonly observed in hormone-stimulated cells using this signaling pathway (14, 15).

**Effects of erythropoietin on membrane potential in human BFU-E derived erythroblasts.** One possible mechanism of erythropoietin-activated  $\text{Ca}^{2+}$  influx is via a voltage-dependent  $\text{Ca}^{2+}$  channel (19). To examine the mechanism of Epo-induced

$\text{Ca}^{2+}$  entry, we evaluated the effects of erythropoietin on membrane potential of human erythroblasts under current-clamp. The mean resting membrane potential was  $-10.9 \pm 1.0$  mV ( $n = 43$ ), with a range of  $-26$  to  $+1$  mV. Addition of erythropoietin (2 U/ml) did not cause significant depolarization (maximal potential change  $8.8 \pm 1.4$  mV,  $n = 8$ ) when compared to Iscove's modified Dulbecco's medium control (maximal potential change  $5.4 \pm 1.8$  mV,  $n = 5$ ).

**Voltage-dependent whole cell currents in human BFU-E derived erythroblasts.** To further evaluate whether erythropoietin modulates the activity of a voltage-dependent channel, current-voltage relationship of human erythroblasts in PBS was studied with depolarizing or hyperpolarizing 100-ms pulses from a holding potential of  $-60$  mV under voltage clamp. With depolarization, we did not observe inward current at the beginning of the pulse and no time-dependent outward current in the late stage (Fig. 4A). In addition, after repolarization to the holding potential, no tail current was observed. Addition of erythropoietin at doses (2 U/ml) that maximize  $[\text{Ca}_i]$  increase (1, 2) and  $\text{Ca}^{2+}$  influx did not reveal any voltage-dependent channel activity (data not shown).

**Ionomycin-induced whole cell currents.** Since erythropoietin increased  $[\text{Ca}_i]$  in day 10 human erythroblasts (2, 5, Table

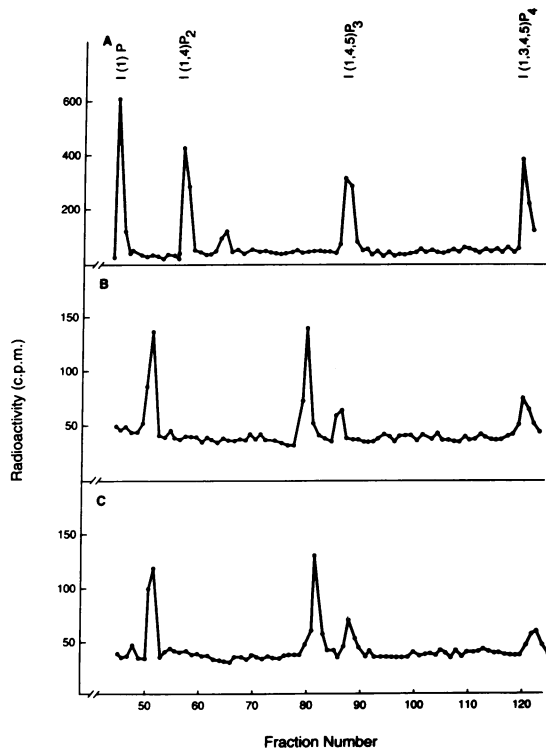


**Figure 3.** Effect of erythropoietin on levels of phosphoinositides in human erythroblasts.  $^3\text{H}$ myo-inositol labeled, day 10 human BFU-E-derived erythroblasts were treated with Epo (10 U/ml) for 5 min and cellular  $^3\text{H}$ inositol phosphates separated by HPLC as described in Methods. (A) Separation of  $^3\text{H}$ inositol phosphates standards. (B) Control. (C) Epo-stimulated cells. Fractions 86–89 eluted with  $^3\text{H}$ inositol-1,4,5-trisphosphate and fractions 120–124 eluted with  $^3\text{H}$ inositol-1,3,4,5-tetrakisphosphate. Fractions 80–83 eluted in the region expected for  $^3\text{H}$ inositol-1,3,4-trisphosphate (15). The peak in fractions 50–53 is unidentified but eluted between  $^3\text{H}$ inositol-1-phosphate and  $^3\text{H}$ inositol-1,4-bisphosphate.

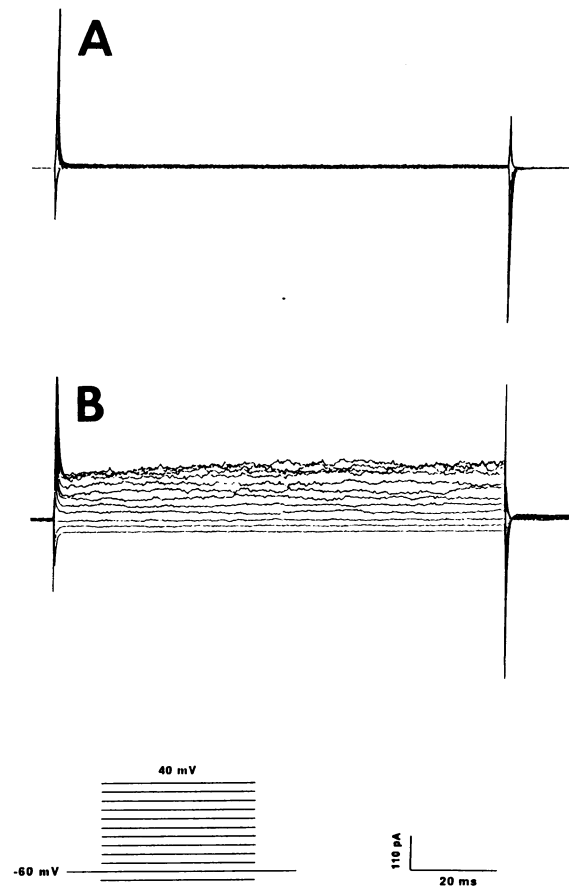


**Figure 4.** Membrane currents in a human BFU-E-derived erythroblast. (A) Whole cell currents in response to 100 ms voltage steps ( $-80$ – $-40$  mV) every 5 s from holding potential of  $-60$  mV. Bath was PBS and normal electrode filling solution was used in these experiments. (B) Same cell after addition of ionomycin (1  $\mu\text{M}$ ). For comparison, the gain was identical in both current traces. (Inset) Stimulus protocol and current and time scale.

II), and since  $\text{Ca}^{2+}$ -activated  $\text{K}^+$  channels have been described in human RBCs (20), we attempted to detect  $\text{Ca}^{2+}$ -activated ion channels in human erythroblasts. To acutely increase  $[\text{Ca}_i]$ , ionomycin ( $1 \mu\text{M}$ ) was added to cells in PBS containing  $0.7 \text{ mM}$   $\text{Ca}^{2+}$ . Addition of ionomycin produced a large increase in outward current (Fig. 4 B) with a shift of reversal potential from  $20$  to  $-70 \text{ mV}$  (Fig. 5).

The shift of reversal potential towards the estimated  $\text{K}^+$  equilibrium potential ( $E_K = -86 \text{ mV}$ ; assuming  $125 \text{ mM}$   $[\text{K}_i]$  and  $4.2 \text{ mM}$   $[\text{K}_o]$  in PBS) suggests that the ionomycin-induced membrane current was mediated by  $\text{K}^+$  efflux rather than  $\text{Cl}^-$  influx (assuming  $E_{\text{Cl}} = -9 \text{ mV}$  as in human RBCs). Indeed, substitution of  $\text{K}^+$  with  $\text{Cs}^+$  in bath and pipette filling solutions abolished the ionomycin-induced membrane current (data not shown). On the other hand, replacement of  $\text{Cl}^-$  with aspartate (KASP) (Table I) had little to no effect on ionomycin-induced membrane currents (Fig. 6). These ion substitution experiments strongly suggest that the ionomycin-induced membrane current was carried by  $\text{K}^+$  rather than  $\text{Cl}^-$  ions. In support of this, when membrane potential was monitored under current-clamp conditions, addition of ionomycin ( $1 \mu\text{M}$ ) to human erythroblasts in PBS rapidly hyperpolarized cells from  $-2.8 \pm 1.9$  to  $-71.5 \pm 4.2 \text{ mV}$  ( $n = 4$ ), which is close to  $E_K$ . In contrast, membrane potential of control cells changed from  $-7.0 \pm 2.7$  to  $-1.6 \pm 1.9 \text{ mV}$  ( $n = 4$ ) during the same period of observation. Typical time courses of membrane potential changes are shown in Fig. 7.

When both extra- and intracellular  $\text{Ca}^{2+}$  were chelated with excess EGTA, addition of ionomycin to human erythroblasts could no longer elicit an increase in membrane current (data not shown), suggesting the ionomycin-induced  $\text{K}^+$  current was  $\text{Ca}^{2+}$  activated. Reversibility of  $\text{Ca}^{2+}$  activation of whole cell current is demonstrated in Fig. 8. In this experiment,  $\text{Ca}^{2+}$  activation of  $\text{K}^+$  channel was well established in a human erythroblast bathed in PBS. Subsequent addition of  $4 \text{ mM}$  EGTA to the same cell abolished the  $\text{Ca}^{2+}$ -activated membrane current.

**Erythropoietin-induced  $[\text{Ca}_i]$  increase and  $\text{Ca}^{2+}$ -activated  $\text{K}^+$  channel.** The maximal increase in  $[\text{Ca}_i]$  of human erythroblasts treated with erythropoietin ( $2 \text{ U/ml}$ ) was  $\sim 200\text{--}300 \text{ nM}$  (1, 2, 5; Table II). To assess whether this magnitude of  $[\text{Ca}_i]$  increase was sufficient to activate  $\text{Ca}^{2+}$ -dependent  $\text{K}^+$  chan-

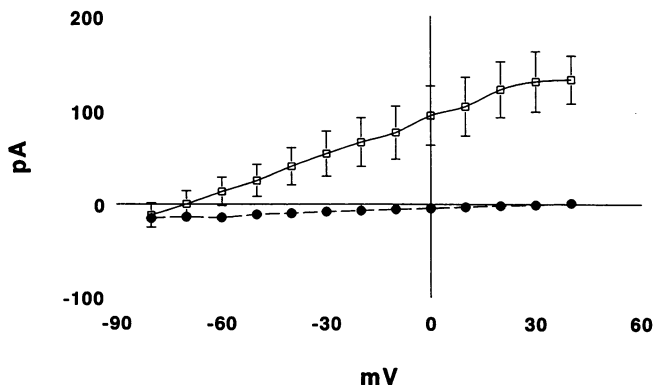


Figure 5. Effects of increased  $[\text{Ca}_i]$  on membrane currents. Experiments were performed as in Fig. 4. Data represent mean  $\pm$  SEM from five cells before ( $\bullet$ ) and after ( $\square$ ) addition of ionomycin ( $1 \mu\text{M}$ ). Note the shift of reversal potential from  $20$  to  $-70 \text{ mV}$  after ionomycin treatment. Average linear slope conductance increased from  $133$  to  $1,250 \text{ pS}$ .

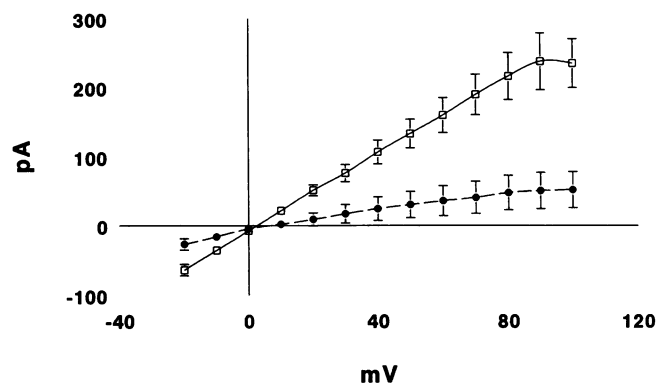


Figure 6. Whole cell currents in symmetrical KASP solution. Symmetrical KASP solutions (Table I) were used to minimize  $\text{Cl}^-$  concentrations both inside and outside the cells. Since the expected reversal potential was  $0 \text{ mV}$ , the stimulus protocol (inset, Fig. 4) was modified so that holding potential was  $0 \text{ mV}$  and command voltage pulses were stepped from  $-20$  to  $100 \text{ mV}$ . Data represent mean  $\pm$  SEM from eight cells before ( $\bullet$ ) and after ( $\square$ ) addition of ionomycin ( $1 \mu\text{M}$ ). Note preservation of  $\text{Ca}^{2+}$ -activated membrane current even when  $\text{Cl}^-$  was severely reduced.

nels, extracellular free  $\text{Ca}^{2+}$  was set to  $300\text{--}400 \text{ nM}$  (PBS with no added  $\text{Ca}^{2+}$  and containing  $5 \mu\text{M}$  Fura-2 free acid;  $363 \text{ nM}$  as measured by Fura-2 fluorescence). Ionomycin ( $1 \mu\text{M}$ ) was then added to erythroblasts to equilibrate extra- and intracellular free  $\text{Ca}^{2+}$  and membrane currents measured under voltage clamp. With extracellular free  $\text{Ca}^{2+}$  at  $363 \text{ nM}$  rather than  $0.7 \text{ mM}$ , ionomycin treatment did not increase whole cell currents in erythroblasts ( $n = 5$ ). In parallel experiments using our digital video imaging system and under similar low extracellular free  $\text{Ca}^{2+}$  conditions, ionomycin treatment increased  $[\text{Ca}_i]$  in Fura-2-loaded erythroblasts (from  $99 \pm 10$  to  $416 \pm 27 \text{ nM}$ ;  $n = 7$ ). This result suggests that at the low extracellular  $\text{Ca}^{2+}$  used in this series of electrophysiologic measurements, ionomycin

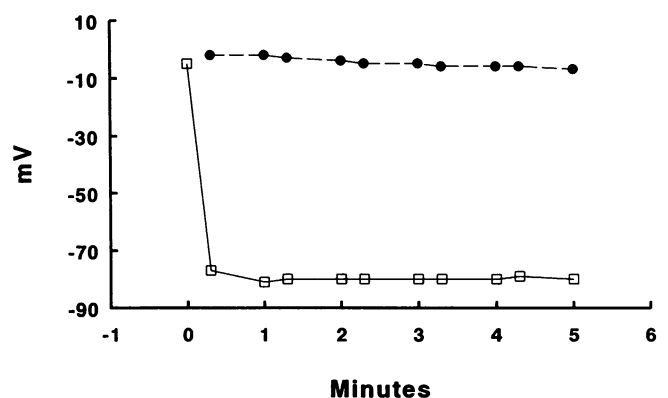
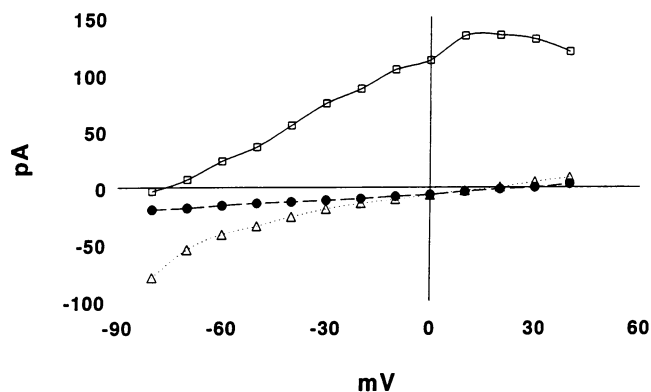


Figure 7. Ionomycin shifts membrane potential toward  $E_K$ . Bath solution was PBS and normal pipette filling solution was used. After rupturing the membrane patch under the electrode tip, holding potential was set to  $-20 \text{ mV}$  and the cell was allowed to stabilize for  $2\text{--}3 \text{ min}$ . The Axopatch-1C amplifier was then switched to the current-clamp mode. After steady-state membrane potential was attained, ionomycin ( $1 \mu\text{M}$ ) was added at time  $0$  to an erythroblast ( $\square$ ). Note immediate shift of membrane potential towards the  $\text{K}^+$  equilibrium potential. Dimethylsulfoxide (ionomycin carrier) was added to another cell as a control ( $\bullet$ ), and no significant membrane potential change was observed.



**Figure 8.** Reversibility of  $\text{Ca}^{2+}$ -activated whole cell currents. Experiment was performed as in Fig. 4. After baseline ( $\bullet$ ) current-voltage relationship was obtained for a human erythroblast in PBS,  $1 \mu\text{M}$  of ionomycin ( $\square$ ) was added.  $\text{Ca}^{2+}$ -activated membrane currents similar to those observed in Fig. 5 were clearly evident. Subsequent addition of  $4 \text{ mM}$  EGTA ( $\Delta$ ) to the same cell completely abolished the  $\text{Ca}^{2+}$ -induced increase in membrane currents.

treatment should have increased  $[\text{Ca}_i]$  to levels similar to those after erythropoietin treatment. We conclude that the magnitude of Epo-induced  $[\text{Ca}_i]$  increase was insufficient to activate  $\text{Ca}^{2+}$ -activated  $\text{K}^+$  channels.

## Discussion

Previous studies by us (1, 2) and others (3) have demonstrated an increase in  $[\text{Ca}_i]$  in human erythroblasts treated with erythropoietin. The increase in  $[\text{Ca}_i]$  was mediated by a pertussis toxin-sensitive G-protein (5), and the  $\text{Ca}^{2+}$  signal was transmitted to the nucleus (8). The relevance of growth factor induced nuclear  $\text{Ca}^{2+}$  increase to cell growth and differentiation is highlighted by the recent finding that the cAMP response element-binding protein is phosphorylated by  $\text{Ca}^{2+}$ -calmodulin-dependent protein kinases I and II and thus functions as a  $\text{Ca}^{2+}$ -regulated transcription factor (21). The mechanism by which  $[\text{Ca}_i]$  increases in response to Epo, however, is not clear.

Two generally accepted mechanisms for  $[\text{Ca}_i]$  increase after receptor occupation include hydrolysis of membrane phosphoinositides (22) and activation of ion channels (19, 23). With respect to Epo-induced  $[\text{Ca}_i]$  increase, the results of our current study indicate that the source of  $\text{Ca}^{2+}$  was entirely derived from extracellular medium, since EGTA obliterated the  $[\text{Ca}_i]$  rise (Fig. 1 and Table II). It could be argued that the lack of  $[\text{Ca}_i]$  increase in Epo-stimulated human erythroblasts incubated in zero  $\text{Ca}^{2+}$  media was caused by the redistribution of intracellular  $\text{Ca}^{2+}$  domains, such that despite a significant increase in  $\text{Ca}^{2+}$  near the submembranous region, the increase was "averaged" out to undetectability when whole cell  $[\text{Ca}_i]$  was calculated. While we cannot categorically rule out this theoretical possibility, the homogeneous appearance of  $\text{Ca}^{2+}$  images taken at cell center plane makes this explanation unlikely, given the spatial resolution limit ( $0.5 \mu\text{m}$ ) of our digital video imaging system with its ability to detect subcellular  $\text{Ca}^{2+}$  gradients (8). It is also unlikely that we would have missed the initial  $\text{Ca}^{2+}$  transient due to  $\text{IP}_3$ , given the temporal resolution (267 ms) of our digital video imaging system. Indeed, the observation that there was no detectable increase in  $\text{IP}_3$  levels in Epo-treated cells (Fig. 3) lends further support to our interpretation that

$[\text{Ca}_i]$  increase was caused by  $\text{Ca}^{2+}$  influx rather than intracellular  $\text{Ca}^{2+}$  release.

$\text{Ca}^{2+}$  influx into Epo-treated erythroblasts was blocked by  $\text{Ni}^{2+}$  (Fig. 2) and moderately high doses of nifedipine (Table III), suggesting that the putative  $\text{Ca}^{2+}$  influx pathway involved in signal transduction of erythropoietin was an ion channel but unlikely to be a voltage-dependent L-type  $\text{Ca}^{2+}$  channel (19). Indeed, addition of Epo did not cause a significant change in membrane potential (Results). Taken together, our results suggest that Epo-induced  $\text{Ca}^{2+}$  influx was mediated via a voltage-insensitive ion channel permeable to  $\text{Ca}^{2+}$ .

The resting membrane potential ( $E_m$ ) of day 10 human BFU-E-derived erythroblasts of  $-11 \text{ mV}$  (Results) is similar to  $-9 \text{ mV}$  measured in human RBCs with potential-sensitive fluorescent probes (24), and  $-8.5 \text{ mV}$  estimate based on intracellular pH measurements (25). The close agreement between the measured  $E_m$  and the theoretical  $\text{Cl}^-$  equilibrium potential ( $E_{\text{Cl}} = -9 \text{ mV}$ ) (24, 25) is consistent with but does not unequivocally prove the hypothesis that in human erythroblasts, permeability to  $\text{Cl}^-$  is much higher than that to  $\text{Na}^+$  or  $\text{K}^+$ . Over the range of voltage clamp applied ( $-80$  to  $+40 \text{ mV}$ ), we did not detect the existence of any voltage-dependent channel activity (Fig. 4). Absence of voltage-dependent channels has been reported in some nonexcitable cells such as rat hepatocytes (26), but not in others such as human neutrophils (27) and lymphocytes (28). With respect to hematopoietic cells of red cell lineage, Hamill (29) reported  $\text{K}^+$  selective channels that were not voltage-dependent in human RBCs.

Since erythropoietin increases  $[\text{Ca}_i]$  from a baseline of  $20\text{--}40 \text{ nM}$  to  $200\text{--}300 \text{ nM}$  (1, 2, 5, 8; Table II), we investigated if ion channels would be activated by increases in  $[\text{Ca}_i]$ . Using ionomycin to "equilibrate" extra- and intracellular  $\text{Ca}^{2+}$ , we detected  $\text{Ca}^{2+}$ -activated  $\text{K}^+$  channels in human erythroblasts.  $\text{Ca}^{2+}$ -activated  $\text{K}^+$  channels have been described in a wide variety of cells (30) including human RBCs (20, 25) and are responsible for the Gardos effect (31). In human red blood cells,  $\text{Ca}^{2+}$ -activated  $\text{K}^+$  channels are voltage independent, charybdotoxin sensitive, and typically of small ( $20\text{--}40 \text{ pS}$ ) single channel conductances (20, 25, 30). The number of  $\text{Ca}^{2+}$ -activated  $\text{K}^+$  channels per human RBC has been estimated to be  $1\text{--}55$ , based on unitary conductance,  $\text{Rb}^+$  efflux measurements, and assuming "mean" channel open probability of  $0.5$  (20);  $0.6\text{--}2$  channels per cell based on  $V_{\text{max}}$  values of charybdotoxin-sensitive,  $\text{Ca}^{2+}$ - $\text{K}^+$  efflux (25); to  $100\text{--}200$  channels per RBC based on  $^{86}\text{Rb}^+$  release from inside-out plasma membrane vesicles (32). While we did not measure directly the number of  $\text{Ca}^{2+}$ -activated  $\text{K}^+$  channels on a human erythroblast, we have demonstrated clearly that when fully activated, the number and/or conductance of these channels were sufficient to move  $E_m$  towards  $E_{\text{K}}$  (Fig. 7). This is in contrast to the conclusion of Wolff et al. (25), based on their observations with human RBCs. The physiological role of  $\text{Ca}^{2+}$ -activated  $\text{K}^+$  channels in human RBCs or human erythroblasts, however, remains undefined. More recently,  $\text{Ca}^{2+}$ -activated  $\text{K}^+$  channels have been used as experimental markers for receptor-induced  $[\text{Ca}_i]$  increase (33, 34). Indeed, in rat pituitary gonadotropes, stimulation with gonadotropin-releasing hormone increased  $[\text{Ca}_i]$  rhythmically with corresponding periodic opening of  $\text{Ca}^{2+}$ -activated  $\text{K}^+$  channels, resulting in oscillations in membrane current and rhythmic hyperpolarization (33). An important finding of the current study, therefore, is that at  $[\text{Ca}_i]$  levels typically found in Epo-treated erythroblasts,  $\text{Ca}^{2+}$ -activated  $\text{K}^+$  channels were not activated.

In the current series of experiments, we did not attempt to detect the Epo-regulatable  $\text{Ca}^{2+}$  channel in human erythroblasts using the whole cell patch-clamp configuration. Based on an estimated erythroblast volume of 0.5 pl (assuming a perfect sphere with a diameter of 10  $\mu\text{m}$ ) (8), and a  $[\text{Ca}_i]$  increase rate of 100 nM/min (based on Fura-2 measurements; 2), the calculated  $\text{Ca}^{2+}$  current/cell would have been  $1.7 \times 10^{-4}$  pA. This current magnitude is too low to be detectable by the whole cell patch-clamp configuration. Even allowing for the differences between  $^{45}\text{Ca}^{2+}$  influx rate (unidirectional flux) and rate of  $[\text{Ca}_i]$  increase as detected by Fura-2 fluorescence (net  $\text{Ca}^{2+}$  flux—intracellular organelle sequestration—intracellular  $\text{Ca}^{2+}$  binding), the resultant estimated  $\text{Ca}^{2+}$  current/cell would still be at the lower limit of detection using the current whole cell configuration. Single channel recording techniques (16) may offer the requisite sensitivity to detect the activity of Epo-regulatable ion channels in the future. Indeed, recent application of single channel recording methodology revealed a voltage-insensitive, receptor-mediated  $\text{Ca}^{2+}$ -entry pathway in cultured endothelial cells (35).

In summary, we have demonstrated by single cell  $\text{Ca}^{2+}$  and electrophysiologic measurements that erythropoietin modulates a voltage-independent  $\text{Ca}^{2+}$  channel in human erythroblasts. Opening of this  $\text{Ca}^{2+}$  channel, rather than intracellular  $\text{Ca}^{2+}$  mobilization by  $\text{IP}_3$ , virtually accounts for the observed increase in  $[\text{Ca}_i]$  in Epo-treated erythroblasts. The magnitude of Epo-induced  $[\text{Ca}_i]$  increase, however, was not sufficient to open  $\text{Ca}^{2+}$ -activated  $\text{K}^+$  channels in erythroblasts. Finally, no voltage-dependent channel activity was detected in human erythroblasts.

## Acknowledgments

The authors would like to thank Tracey Erickson for assistance in the preparation of the manuscript.

This work was supported in part by National Institutes of Health grants HL-40576, HL-40306, HL-41582, HL-43215, DK-40069, and DK-40127; Biomedical Research Support Grant Program, Division of Research Resources, grant SO7-RR-05680-21; and American Heart Association (Pennsylvania Affiliate) Grant-in-Aid. Dr. Miller is the recipient of a Junior Faculty Award from the American Cancer Society.

## References

1. Miller, B. A., R. C. Scaduto, Jr., D. L. Tillotson, J. J. Botti, and J. Y. Cheung. 1988. Erythropoietin stimulates a rise in intracellular free calcium concentration in single early human erythroid precursors. *J. Clin. Invest.* 82:309–315.
2. Miller, B. A., J. Y. Cheung, D. L. Tillotson, S. M. Hope, and R. C. Scaduto, Jr. 1989. Erythropoietin stimulates a rise in intracellular-free calcium concentration in single BFU-E derived erythroblasts at specific stages of differentiation. *Blood.* 73:1188–1194.
3. Mladenovic, J., and N. E. Kay. 1988. Erythropoietin induces rapid increases in intracellular free calcium in human bone marrow cells. *J. Lab. Clin. Med.* 112:23–27.
4. Bonanou-Tzedaki, S. A., M. S. Setchenska, and H. R. V. Arnstein. 1986. Stimulation of the adenylate cyclase activity of rabbit bone marrow immature erythroblasts by erythropoietin and haemin. *Eur. J. Biochem.* 115:363–370.
5. Miller, B. A., K. Foster, J. D. Robishaw, C. F. Whitfield, L. Bell, and J. Y. Cheung. 1991. Role of pertussis toxin-sensitive GTP-binding proteins in the response of erythroblasts to erythropoietin. *Blood.* 77:486–492.
6. Choi, H. S., D. M. Wojchowski, and A. J. Sytkowski. 1987. Erythropoietin rapidly alters phosphorylation of pp43 on erythroid membrane protein. *J. Biol. Chem.* 262:2933–2936.
7. Hilton, C. J., A. S. Tan, and M. V. Berridge. 1989. Evidence for direct involvement of G-proteins in erythropoietin signal transduction. *Blood.* 74(Suppl. 1):193a.
8. Yelamarty, R. V., B. A. Miller, R. C. Scaduto, Jr., F. T. S. Yu, D. L. Tillotson, and J. Y. Cheung. 1990. Three-dimensional intracellular calcium gradients in single human burst-forming units-erythroid-derived erythroblasts induced by erythropoietin. *J. Clin. Invest.* 85:1799–1809.
9. Mason-Garcia, M., C. L. Weill, and B. S. Beckman. 1990. Rapid activation by erythropoietin or protein kinase C in nuclei of erythroid progenitor cells. *Biochem. Biophys. Res. Commun.* 168:490–497.
10. Corbet, J.-F., M.-T. Mitjavila, A. Dubart, D. Roten, S. C. Weil, and W. Vainchenker. 1989. Expression of the c-fos protooncogene by human and murine erythroblasts. *Blood.* 74:947–951.
11. Prochownik, E. V., M. J. Smith, K. Snyder, and D. Emeagwali. 1990. Amplified expression of three jun family members inhibits erythroleukemia differentiation. *Blood.* 76:1830–1837.
12. Todokoro, K., R. J. Watson, H. Higo, H. Amamuma, S. Kuramochi, H. Yanagisawa, and Y. Ikawa. 1988. Down-regulation of c-myc gene expression is a prerequisite for erythropoietin-induced erythroid differentiation. *Proc. Natl. Acad. Sci. USA.* 85:8900–8904.
13. Grynkiewicz, G., M. Poenie, and R. Y. Tsien. 1985. A new generation of  $\text{Ca}^{2+}$  indicators with greatly improved fluorescence properties. *J. Biol. Chem.* 260:3440–3450.
14. Dean, N. M., and J. D. Moyer. 1987. Separation of multiple isomers of inositol phosphates formed in  $\text{GH}_3$  cells. *Biochem. J.* 242:361–366.
15. Hansen, C. A., S. Mak, and J. R. Williamson. 1986. Formation and metabolism of inositol 1,3,4,5-tetrakisphosphate in liver. *J. Biol. Chem.* 261:8100–8103.
16. Hamill, O. P., A. Marty, E. Neher, B. Sakman, and F. Sigworth. 1981. Improved patch-clamp techniques for high-resolution current recording from cells and cell-free membrane patches. *Pfluegers Arch. Eur. J. Physiol.* 391:85–100.
17. Leibowitz, M. D., and V. E. Dionne. 1987. A polisher for patch pipettes. *Pfluegers Arch. Eur. J. Physiol.* 410:338–339.
18. Hagiwara, S., and H. Ohmori. 1982. Studies of calcium channels in rat clonal pituitary cells with patch electrode voltage clamp. *J. Physiol. (Lond.)* 331:231–252.
19. Tsien, R. W., and R. Y. Tsien. 1990. Calcium channels, stores, and oscillations. *Annu. Rev. Cell Biol.* 6:715–760.
20. Grygorczyk, R., W. Schwarz, and H. Passow. 1984.  $\text{Ca}^{2+}$ -activated  $\text{K}^+$  channels in human red cells. *Biophys. J.* 45:693–698.
21. Sheng, M., M. A. Thompson, and M. E. Greenberg. 1991. CREB: a  $\text{Ca}^{2+}$ -regulated transcription factor phosphorylated by calmodulin-dependent kinases. *Science (Wash. DC)* 252:1427–1430.
22. Berridge, M. J. 1988. Inositol lipids and calcium signalling. *Proc. R. Soc. Lond. B Biol. Sci.* 234:359–378.
23. Brown, A. M., and L. Birnbaumer. 1988. Direct G protein gating of ion channels. *Am. J. Physiol.* 254(Heart Circ. Physiol.) 23:H401–H410.
24. Hoffman, J. F., and P. C. Harris. 1974. Determination of membrane potentials in human and Amphiuma red blood cells by means of a fluorescent probe. *J. Physiol. (Lond.)* 239:519–552.
25. Wolff, D., X. Cecchi, A. Spalvin, and M. Canessa. 1988. Charybdotoxin blocks with high affinity the  $\text{Ca}^{2+}$ -activated  $\text{K}^+$  channel of Hb A and Hb S red cells: individual differences in the number of channels. *J. Membr. Biol.* 106:243–252.
26. Sawanobori, T., H. Takanashi, M. Hiraoka, Y. Ida, K. Kamisaka, and H. Maezawa. 1989. Electrophysiological properties of isolated rat liver cells. *J. Cell. Physiol.* 139:580–585.
27. Krause, K.-H., and M. J. Welsh. 1990. Voltage-dependent and  $\text{Ca}^{2+}$ -activated ion channels in human neutrophils. *J. Clin. Invest.* 85:491–498.
28. Lewis, R. S., and M. D. Cahalan. 1990. Ion channels and signal transduction in lymphocytes. *Annu. Rev. Physiol.* 52:415–430.
29. Hamill, O. P. 1981. Potassium channel current in human red blood cells. *J. Physiol. (Lond.)* 319:97–98P.
30. Latorre, R., A. Oberhauser, P. Lebarrea, and O. Alvarez. 1989. Varieties of calcium-activated potassium channels. *Annu. Rev. Physiol.* 51:385–399.
31. Gardos, G. 1958. The function of calcium in the potassium permeability of human erythrocytes. *Biochim. Biophys. Acta.* 30:653–654.
32. Lew, V. L., S. Muallem, and C. A. Seymour. 1982. Properties of the  $\text{Ca}^{2+}$ -activated  $\text{K}^+$  channel in one-step inside-out vesicles from human red cell membranes. *Nature (Lond.)* 296:742–744.
33. Tse, A., and B. Hille. 1992. GnRH-induced  $\text{Ca}^{2+}$  oscillations and rhythmic hyperpolarization of pituitary gonadotropes. *Science (Wash. DC)* 255:462–464.
34. Bird, G. St. J., M. F. Rossier, A. R. Hughes, S. B. Shears, D. L. Armstrong, and J. W. Putney, Jr. 1991. Activation of  $\text{Ca}^{2+}$  entry into acinar cells by a non-phosphorylatable inositol trisphosphate. *Nature (Lond.)* 352:162–165.
35. Luckhoff, A., and D. E. Clapham. 1992. Inositol 1,3,4,5-tetrakisphosphate activates an endothelial  $\text{Ca}^{2+}$ -permeable channel. *Nature (Lond.)* 355:356–358.